TRIUMF — RESEARCH PROPOSAL	Experiment no. 742	Sheet 1 of 28

Title of proposed experiment:

Scattering of Muonic Hydrogen Isotopes

Name of group: Muonic Hydrogen

Spokesperson for group: V.M. Bystritsky, R. Jacot-Guillarmod, F. Mulhauser

E-Mail address: mulhauser@erich.triumf.ca Fax number: (604)-222-1074

Members of the group (name, institution, status, per cent of time devoted to experiment)

Name	Institution	Status	Time
V.M. Bystritsky	JINR	Senior Researcher	60%
R. Jacot-Guillarmod	University of Fribourg	Research Scientist	50%
F. Mulhauser	TRIUMF	Research Associate	50%
J. Wozniak	Inst. Phys. Nucl. Tech. Cracow	Assistant Professor	50%
V.A. Stolupin	JINR	Senior Researcher	50%
W. Czaplinski	Univ. Mining & Metallurgy Cracow	Research Scientist	40%
M. Filipowicz	Univ. Mining & Metallurgy Cracow	Postgraduate Student	40%
A. Adamczak	Inst. Nucl. Physics Cracow	Assistant Professor	25%
A.R. Kunselman	University of Wyoming	Professor	25%
C. Petitjean	PSI	Research Scientist	25%
T.M. Huber	Gustavus Adolphus College	Assistant Professor	25%
V.E. Markushin	Kurtchatov Institute, Moscow	Senior Researcher	20%
L.A. Rivkis	Inst. Inorg. Mat. VNIINM Moscow	Senior Researcher	20%
A. Olin	University of Victoria	Senior Research Scientist	15%
G.M. Marshall	TRIUMF	Research Scientist	10%
P.E. Knowles	University of Victoria	Graduate Student	10%
G.A. Beer	University of Victoria	Professor	10%
P. Kammel	University of California Berkeley	Research Scientist	10%
M.C. Fujiwara	University of British Columbia	Graduate Student	10%
J. Zmeskal	IMEP Vienna	Research Scientist	10%

Start of preparations:	Fall 1994
Date ready:	Summer 1995
Completion date:	Fall 1997

Beam time requested:

12-hr shifts	Beam line/channel	Polarized primary beam?
72	M20B	No

We propose to measure the differential scattering cross sections of the reactions

$$\mu x + H_2 \rightarrow \mu x + H_2 \quad (x = d, t)$$

in the energy collision range from 0.1 to 45 eV. These reactions are especially interesting because of the Ramsauer-Townsend effect which occurs near 6 eV for muonic deuterium and 13 eV for muonic tritium (in lab frame). At these energies, the scattering cross section drops significantly and the interaction length for μx on H_2 increases to a macroscopic scale (order of 1 mm). This explains why muonic deuterium (or tritium) can escape from solid protium-deuterium (or tritium) layers with measurable rates. TRIUMF experiment 453 took advantage of the mechanism to study the rate of emission in terms of deuterium concentration and layer thickness, while experiment 613 focussed on the muonic formation rates of $dd\mu$ and $dt\mu$ molecules. The specific task of this proposal is to measure the energy dependence of the scattering cross sections of muonic deuterium and tritium on hydrogen molecules. The results will be compared with the theoretical calculations [1,2] which have been recently achieved with high accuracy.

A typical experimental setup will consist of a thick, $\sim$ 1 mm, protium-deuterium layer frozen on the surface of the first, called upstream, gold foil. On the second gold foil (called downstream, located at 20 mm from the first one), a neon layer will be sandwiched between the gold foil and a pure protium layer where the muonic atoms will interact. Muonic atoms surviving the drift across the 20 mm of vacuum and not stopping in the downstream protium layer will disappear by muon transfer to neon. The μd drift time from the emitting layer to the protium layer is the dominant contribution to the total time beginning with the μ stop in the protium-deuterium layer and ending with the emission of the neon X-rays as measured by a germanium detector. Hence the time-of-flight method can be applied to determine the collision energy.

Depending on the thickness of the protium layer, different energy ranges of the μd or μt will interact. Measurements of the energy distribution will be performed by inserting a collimation device between the gold foils, which limits the acceptance of the muonic atoms to angles close to perpendicular.

The molecular $pd\mu$ and $pt\mu$ formations, which are non-resonant, are parasitic processes that we will have to understand. Separate measurements will be attempted to experimentally extract their contribution, and to measure effective formation rates for the 0.1 to 45 eV energy range. To do this the 5.5 MeV ($pd\mu$) and 19.8 MeV ($pt\mu$) γ-rays emitted during the fusion processes will be detected using an array of NaI(Tl) crystals.

Experimental area

Meson Hall

Primary beam and target (energy, energy spread, intensity, pulse characteristics, emittance)

> 140 μA unpolarized protons at 500 MeV on 10 cm Be target

Secondary channel M20B

Secondary beam (particle type, momentum range, momentum bite, solid angle, spot size, emmittance, intensity, beam purity, target, special characteristics)

cloud μ^- at $\sim$27 MeV/c, luminosity 5×10^3 or greater in 4 cm diameter, $\Delta p/p \sim 4\%$.

TRIUMF SUPPORT:

1. Test space: The complexity of the system requires that it is set up and tested out of beam to minimize wasted beam time, in a space of roughly 20 m^2 with crane access. So far (*i.e.* for Expt. 613) we used the M20A-leg for this purpose which is very convenient and close to the required channel. Safe hermetic storage for components which have been exposed to tritium gas is necessary. A stack vent and tritium monitoring system will be needed both in the test area and in the M20B beam area during tritium handling. We have purchased one tritium monitor but will require the use of an identical device now owned by the TRIUMF safety group.

2. Financial: In order to allow the Eastern European collaborators to fully participate in the measurements, we require a financial contribution from TRIUMF of $25,000. This amount include the travel cost (reduced to 70% after personnel contributions from the collaborator's institutions), the accommodation at TRIUMF house, and the per diem.

3. Detectors and electronics: three 20×20 cm^2 delay line cathode strip MWPCs, the MINA NaI(Tl) crystal, and two high resolution Ge detectors. NIM and CAMAC electronics and high voltage supplies. VAX-based data acquisition system. The experiment uses a substantial quantity of electronic modules from the Electronics Pool; in the past, some items have been in short supply and we have had to import or purchase some devices to mount the experiment.

4. Other: Liquid helium (500 ℓ per week).

NON-TRIUMF SUPPORT

5 NaI(Tl) crystals from JINR at Dubna, presently located at TRIUMF.

The experiment is funded mostly from NSERC Project Grant IEP-216. Other essential equipment is provided by collaborators from JINR, PSI, IMEP, Wyoming and Fribourg.

The construction of the tritium handling system for this experiment is complete, and it has not presented any essential problems. The tritium is stored in uranium bed from which it can be extracted by heating. After use in the cryogenic target, it is pumped with high efficiency into another bed as a mixture of isotopes. The maximum amount of free elemental tritium within the target system at any given time will be less than 10 Ci (for details see [3]). An independent safety assessment of the 800 Ci target of Experiment 454 [4] derived a release limit of 120 Ci per week, based on exposure to the public of tritium released through the meson hall ventilation stack. In the event of a catastrophic failure (*e.g.* loss of primary vacuum integrity and vaporization of the hydrogen target into the secondary containment), 10 Ci of tritium would be released through the stack.

To ensure that any tritium which escapes in the event of a failure will be exhausted to the ventilation stack, all parts of the apparatus which have any chance of being exposed to tritium are contained within an enclosure which is exhausted by a fan to the stack. The equipment is operable from outside the enclosure. All pumps which may be exposed to tritium are normally exhausted to a large waste volume, which can then be vented to the stack. An automatic interlocked gate valve avoids contamination of the beam line vacuum system.

Tritium monitors are installed to monitor the tritium levels in the exhaust stack and inside and outside the experimental enclosure. Vacuum gauges and thermometers are installed to allow the early detection of leaks or other malfunctions. These monitors will be connected to a programmable logic control (PLC) system to provide interlocks and alarms (for details see [3]).

The safety system and the tritium handling has been reviewed and approved by the TRIUMF Safety Group.

Apart from the radiation hazard posed by tritium, the major difficulty is to prevent explosive mixtures formed from the hydrogen which is to be frozen to the gold foil. The largest target we anticipate contains less than 0.5 g ($\sim$6 ℓ at NTP) of hydrogen. If we suffer an unplanned warming of the foil, the non-explosive mixture in the vacuum system (total volume about 27 ℓ) will stay below atmospheric pressure, so that the integrity of the stainless steel windows remains. When the foils are warmed, either in planned or unplanned circumstances, the pumping system removes the hydrogen gas safely. In any case where tritium is in the target, the storage bed will be used as the pump. A system to allow purging of the mechanical pumping system with nitrogen both before and after pumping hydrogen eliminates the possibility of explosive mixtures of hydrogen and oxygen within the pump and pumping lines.

The only other hazards envisaged are minor and are common to many experiments in which the group has been involved, and are well understood. These include the use of MWPC gas and high voltage systems, scintillator high voltage, and liquid helium.

1 Scientific Justification

There are many interactions of a negative muon stopped in a mixture of hydrogen isotopes. The formation of muonic atoms and molecules occur as branches of these interactions. These formation reactions take place before any nuclear reactions such as fusion or muon capture [5,6]. Preceding the molecular formation reaction are scattering reactions of the muonic atoms which change their state and hence affect the formation reactions. In particular, the knowledge of cross sections for scattering of μp, μd and μt to molecules of hydrogen isotopes is necessary not only for checking the algorithmic solution of the Coulomb three-body problem but also for a general and correct description of the kinetics of muons in nuclear fusion reactions. The cross sections are also required for a correct interpretation of the results from experiments which aim to determine the weak interaction constants in the case of the nuclear capture rate of the muon by a proton, deuteron, or triton, since the nuclear capture rate depends on the population of the hyperfine levels of the hydrogen atom [7,8].

Much theoretical research [1,2,9–13] has been devoted to the calculation of the cross sections for scattering of μp, μd and μt atoms on protons, deuterons, tritons and on hydrogen isotope molecules. Much less has been done to study the scattering experimentally. Experimental scattering cross sections exist only for μp atoms in hydrogen [14–17] and for μd atoms in deuterium [15,16,18,19]. There is a discrepancy between the experimental results of references [15–17] and of references [14,18,19] as well as between the experimental results and theoretical findings [1,10–13].

The cause of the substantial discrepancy between the sets of measured cross sections is not yet clear. The results of a recent investigation of the processes

$$\mu p + \mathrm{H}_2 \quad \rightarrow \quad \mu p + \mathrm{H}_2, \tag{1}$$

by the collaboration Williamsburg-PSI-Vienna-Mississippi-Munich [20–22] are also still far from good agreement with calculations. The analysis of the experimental data continues in collaboration with theorists. A similar experiment for the deuterium case

$$\mu d + \mathrm{D}_2 \quad \rightarrow \quad \mu d + \mathrm{D}_2, \tag{2}$$

performed by the same group, agrees well with the recent Monte Carlo simulations [23]. However, the magnitude of the calculated cross sections is checked using only a single scaling parameter for the interval $0 - 50$ eV. That does not give direct information about the energy dependence of the cross sections. Moreover, the results depend on the assumed initial distribution of μd energy.

As to the process of μd and μt atoms scattering in hydrogen via reactions

$$\mu d + \mathrm{H}_2 \rightarrow \mu d + \mathrm{H}_2, \tag{3}$$

$$\mu t + \mathrm{H}_2 \rightarrow \mu t + \mathrm{H}_2, \tag{4}$$

there is clear evidence for the Ramsauer-Townsend effect in diffusion data [24,25], but no detailed information about the energy dependence of the cross section of (4) and only the upper estimate for the cross section of (3) are available [18–21,26]. The knowledge of the cross sections for (3) and (4) is necessary for a correct description of the kinetics of μ-atomic

and μ-molecular processes in H_2+D_2, H_2+T_2 and H_2+D_2+T_2 mixtures. It is also required for the interpretation of experiments of the muon capture rate by a deuteron or triton, and for verifying the algorithm of the cross section calculations of (3) and (4). It follows from theoretical findings [1,2,11,12,27] that the Ramsauer-Townsend effect may take place in elastic scattering of μd and μt atoms from H_2 molecules. The Ramsauer-Townsend effect makes the scattering cross section extremely small ($\sim 10^{-21}$ cm^2) at collision energies of $2 - 20$ eV (see Fig. 1) when compared to other energy values of the cross section ($\sim 10^{-19}$ cm^2).

Traditionally [28–31], the scattering cross section was deduced from the diffusion length in hydrogen (deuterium, tritium, or mixtures thereof) by making use of Monte Carlo simulations. The Monte Carlo depends highly on certain assumptions made about the process being simulated. The assumptions deal with the energy distribution of the muonic atoms, the dependence of the cross section on the collision energy, the angular distribution of muonic atoms scattered from the hydrogen isotope molecules, and the energy dependence of cross sections for competing processes (*e.g.* muon transfer from light to heavy hydrogen isotopes and from hydrogen isotopes to $Z > 1$ impurities, the formation of muonic molecules and spin flip).

For correct comparison of experimental results with theoretical calculations of μ-atom scattering cross sections one has to set up the experiment in such a way that the Monte Carlo analysis of the experimental data would include as few assumptions as possible. Such a step will obviously increase the reliability of the results.

The technique of producing beams of μd or μt atoms emitted into vacuum [32,33] has an important advantage for the cross section measurements. The time of flight method gives the information on the initial energy of the muonic atom, a previously assumed quantity. The Ramsauer-Townsend effect in the cross section of process (3) and (4) can be investigated as a function of energy. It should be stressed that the energy region (0.1-45 eV) accessible to the emitted μ-atom method is unique and can not be easily seen in diffusion measurements [28–31]. The advantages of the beam technique are as follows :

1. It is possible to produce pure beams of neutral μd or μt from a H_2 + 0.1% D_2 (resp. T_2) layer on the upstream gold foil surface which are emitted into vacuum with a known energy distribution. In our opinion, the apparatus (Fig. 2) developed at TRIUMF (Expt. 613) [33] to study $dt\mu$ and $dd\mu$-fusion reactions [34–36] is very promising for the measurement of the scattering cross sections of μd and μt atoms on H_2 molecules.

2. A direct test of the predicted energy dependence in the region of the Ramsauer-Townsend effect in cross sections for scattering of μd and μt atoms from hydrogen molecules and a correct measurement of cross sections for reactions (3) and (4) is achievable. Quantitative interpretation of the traditional diffusion experiments is highly ambiguous because it requires a precise knowledge of the cross sections of competing processes which may exceed cross sections for processes (3) and (4).

3. One can verify the theoretical dependence of differential scattering cross sections of μd and μt atoms on H_2 molecules for collision energies in the range $0.1 - 45$ eV.

4. It may be possible to measure the effective rate for $pd\mu$ and $pt\mu$ molecular formation

in the collision energy range 0.1 – 45 eV and to verify the theoretical calculation [37].

Finally, it should be mentioned that this method can be applied to the cross section measurement of scattering of μd or μt atoms on D_2 or T_2 molecules in the same energy range.

2 Description of the Experiment

Experiments 453 and 613 have shown that we can extract neutral beams of μd and μt atoms into vacuum with energies ranging from about 0.1 to 45 eV. The apparatus we plan to use is the one built for Expt. 613 [33]. Because the basics are very similar, we will present some features which are common with Expt. 613, and those which are specific to this proposal.

The apparatus [34] is shown schematically in Fig. 2. Incident muons of momentum 27 MeV/c ($\Delta p/p = 0.04$ FWHM) are detected by a 0.127 mm scintillator before passing through a 0.025 mm stainless steel vacuum isolation window. The muons continue to lose energy while entering the cryostat and passing through the 70 K heat shield to stop in the hydrogen target or the 0.051 mm gold 3 K target support foils. The μ^- forms muonic protium (μp) and then transfers with high efficiency to a deuteron (μd) or a triton (μt). In the case of muonic deuterium, it obtains a kinetic energy of about 45 eV mainly determined by the recoil due to the difference of the binding energies of μd and μp. The μd loses energy through elastic collisions, mainly with protium, until it reaches about 16 eV, when the calculated cross section $\sigma^{el}_{\mu d+H_2}$ falls below 10^{-20} cm^2 (see Fig. 1) [1,2]. The mean distance between collisions becomes very large, especially at 4 – 12 eV, and the hydrogen layer becomes almost transparent to μd. This is an example of the Ramsauer-Townsend effect noticed in early bubble chamber experiments when muon catalyzed fusion was first observed in the p-d system [24]. The muonic atom is then emitted from the surface into the adjacent vacuum and may reach the downstream layer (pure protium in this case).

Hydrogen (or neon) is deposited on one of the gold surfaces through a diffusion system made of sintered material of 2 μm porosity. The diffuser is inserted from below and can be used to deposit on the two separate cold foils. The gas, which slowly passes through the diffuser, freezes onto the gold foil surface maintained at 3 K. The thickness of the solid hydrogen is controlled by adjusting the amount of hydrogen gas injected. The concentration of the different isotopes of the mixture is made in the gas handling system and monitored during the deposition itself. The hydrogen and neon layer thickness and uniformity has been measured independently via energy loss of alpha particles [38]. Inhomogeneous targets can be made, in which the frozen material consists of different layers containing different hydrogen isotopes or mixtures of isotopes, or even other materials such as neon.

For the measurements we propose, the upstream gold foil will support an emitting layer consisting of 7.0 mg $\cdot$ cm^{-2} ($\sim$0.8 mm) solid hydrogen with one part per thousand deuterium or tritium (which would give about 6 Ci of tritium). The thickness of this layer was chosen large enough to efficiently prevent the direct muon stop in the downstream pure protium layer. The emitting layer is the source of muonic deuterium (or tritium) atoms, which travel toward the adjacent downstream gold foil, and may pass through a

collimation device which limits the transmitted muonic atoms to angles perpendicular to the surface. The collimator is fixed to the top edge of the diffuser mechanism so that it can be inserted and withdrawn easily. The energy distribution of the emitted particles can be changed by adding a very thin D_2 overlayer (*e.g.* 20 $\mu g \cdot cm^{-2}$) on the upstream emitting layer (see Fig. 3). The downstream gold foil is parallel to the upstream foil, separated by 20 mm and supports a target of pure neon (about 2 $mg \cdot cm^{-2}$).

We can determine the energy distribution of the μd or μt atoms reaching the neon layer (Figs. 4 and 5) by measuring the time distribution of the delayed muonic neon X-rays resulting from the muon transfer to the Ne nuclei (Figs. 6 and 7). The time of the appearance of the neon X-ray is dominated by the time needed for μd or μt to cross the known distance between the upstream and downstream foils. Ambiguity in the flight distance resulting from the emission angle of the muonic atom can be constrained by the use of a collimator (see Fig. 8). With the known energy distribution, one can proceed to measure the effect of scattering.

A layer of solid H_2 is deposited on the Ne layer. In this case only a fraction of the initial number of incident μd or μt atoms can reach the Ne layer due to scattering and diffusion in the H_2 layer. Experimentally we measure the ratio

$$\alpha_{dif}^{exp} = \frac{N_\gamma^{reg}(H_2 \oplus Ne)}{N_\gamma^{reg}(Ne)} , \tag{5}$$

as a function of flight time and hence energy. $N_\gamma^{reg}(Ne)$, $N_\gamma^{reg}(H_2 \oplus Ne)$ are the yields of delayed X-rays from μNe atoms measured with Ne and $H_2 \oplus$ Ne layers on the downstream gold foil. The ratio α_{dif}^{exp} is a function of the cross section and the energy, and represents the fraction of the μd atoms that reached the Ne layer by diffusion in the H_2 layer. The effect of the H_2 overlayer in the energy and time distribution was simulated with Monte Carlo and the results are shown in Figs. 4, 5 and 7. The reduction of the time (Fig. 7) with increasing thickness of H_2 is due to the Ramsauer-Townsend effect which allows the fast atoms to travel through the overlayer while the slow component is stopped. A formula similar to (5) can be obtained for μt emission.

Thus, comparing the experimental value of α_{dif}^{exp} with α_{dif}^{theor} obtained by the simulation of the processes induced by μd or μt atoms in the H_2 layer, we can check the energy dependence of the cross section of these atoms scattering on H_2 molecules in a certain energy range. By varying the composition of the emitting layer we can verify the theoretical dependence $\sigma(\mu d + H_2)$ (resp. $\sigma(\mu t + H_2)$) for another collision energy distribution (Fig. 3).

Using chi-square analysis we will verify the calculated cross sections for the scattering processes. If the existing theoretical calculations prove to be unsatisfactory, we can still give information about the scattering cross section as a function of energy. We can give effective cross sections for different energy intervals or by comparing the direct experimental cross section to the theoretical one, we can describe their shortcomings.

In the experiment we hope to be able to measure simultaneously the time distributions and the yields of γ-ray from the $pd\mu$ and $pt\mu$ fusion reactions

$$\begin{aligned} pd\mu \quad &\rightarrow \quad \mu^3He + \gamma \quad (E_\gamma = 5.5\,MeV) \\ &\qquad\quad {}^3He + \mu \quad (E_\mu = 5.3\,MeV), \end{aligned} \tag{6}$$

$$
\begin{aligned}
pt\mu \;\rightarrow\; & \mu^4He + \gamma \;\; (E_\gamma = 19.8\,\mathrm{MeV}) \\
& {}^4He + \mu + \gamma \;\; (E_\gamma = 19.8\,\mathrm{MeV}) \\
& \mu^4He + e^+e^- \;\; (Q = 18.8\,\mathrm{MeV}) \\
& {}^4He + \mu_{conv} \;\; (E_\mu = 19.2\,\mathrm{MeV}),
\end{aligned} \tag{7}
$$

since these data will remove another assumption from the Monte Carlo. The γ-ray must be used since the kinetic energy of the helium nucleus is only a few hundred keV, which is too low for efficient registration using silicon detectors as used by Expt. 613. The γ-rays of $pd\mu$-fusion at 5.5 MeV are emitted with a branching ratio $> 85\%$ (85% for J=0 spin state and higher for other spin states [30,39]). For the 19.8 MeV γ-ray of $pt\mu$-fusion the branching ratio is $> 95\%$ (100% for J=$\frac{3}{2}$ and J=$\left(\frac{1}{2}\right)'$ spin state and about 74% for J=$\frac{1}{2}$ [40]).

For sake of simplicity, and because the technique is the same for μd and μt atoms, we will restrict the following presentation to the case of μd emission. The $pd\mu$ fusion process has been studied in other experiments [30,39–41]. By using the previous experimental fusion rate, we will get information on the effective rate of $pd\mu$ molecular formation for the collision energy range chosen in accordance with the experimental conditions. The yields of the γ-ray in the run with pure H_2 (Y_γ) is :

$$
Y_\gamma \;=\; N_\mu \cdot \varepsilon_{del-e} \cdot \varepsilon_\gamma^{pd} \left(\frac{\varphi \tilde{\lambda}_{pd\mu}}{\lambda_0 + \varphi \tilde{\lambda}_{pd\mu}} \right) \left(\frac{\tilde{\lambda}_{f,\gamma}^{pd}}{\lambda_0 + \tilde{\lambda}_f^{pd}} \right), \tag{8}
$$

where N_μ is the number of participating muons, ε_{del-e} is the delayed electrons condition efficiency, ε_γ^{pd} is the recording efficiency of the $pd\mu$-fusion γ-ray, $\tilde{\lambda}_{pd\mu}$ is the effective molecule $pd\mu$ formation rate averaged on the energy interval 0.1 – 45 eV, $\tilde{\lambda}_f^{pd}$ is the effective nuclear fusion rate of $pd\mu$-molecules, $\tilde{\lambda}_{f,\gamma}^{pd}$ is the effective nuclear fusion rate of $pd\mu$-molecules with γ-ray emission, λ_0 is the free muon decay rate and φ is solid density with respect to the liquid hydrogen density.

From our actual knowledge, we are not able to say if this measurement of the $pd\mu$-molecular formation rate can be done because of rate limitations. In the case of a positive test measurement, we may get independent information of the effective rate of $pd\mu$ molecular formation and on the effective rate of the fusion reaction by performing a set of measurements with a solid homogeneous H_2 + Ne layer on the downstream foil. The yield (Y_γ^*) of the γ-ray in the run with the mixture H_2 + Ne is then,

$$
Y_\gamma^* \;=\; N_\mu \cdot \varepsilon_{del-e} \cdot \varepsilon_\gamma^{pd} \left(\frac{\varphi \tilde{\lambda}_{pd\mu}}{\lambda_0 + \varphi \tilde{\lambda}_{pd\mu} + \varphi c_{Ne} \tilde{\lambda}_{dNe}} \right) \left(\frac{\tilde{\lambda}_{f,\gamma}^{pd}}{\lambda_0 + \tilde{\lambda}_f^{pd}} \right), \tag{9}
$$

where $\tilde{\lambda}_{dNe}$ is the effective transfer rate to Ne and c_{Ne} is the relative atomic concentration of Ne in the mixture H_2 + Ne. One has to notice that the term $\tilde{\lambda}_{f,\gamma}^{pd}/(\lambda_0 + \tilde{\lambda}_f^{pd})$ in the equations (8, 9) is independent of the neon concentration. By varying the Ne concentration (from 3×10^{-5} to 10^{-4}) and measuring the yields and the time distributions of $pd\mu$-fusion γ-rays and muonic neon X-rays, one can find $\tilde{\lambda}_{pd\mu}$, $\tilde{\lambda}_f^{pd}$ and $\tilde{\lambda}_{dNe}$. The latter is also interesting because there is no experimental result for the whole collision energy range.

An imaging system consisting of three multiwire proportional chambers plus scintillators and the NaI crystals determine the time, the energy, and spatial coordinates of the muon decay electron (see Fig. 2). The coordinates are extrapolated back to a perpendicular plane bisecting the target, providing an estimate for the position of the muon at the time of decay.

The fusion γ-rays will be detected by NaI(Tl) detectors placed downstream and on the beam-right arm, just behind the wire chambers (see Fig. 2). The detection efficiency for $pd\mu$-fusion γ-rays (5.5 MeV) is found by measuring the muon gold X-ray yield corresponding to the transition $2p \rightarrow 1s$ (μAu(2p-1s) are at 5.6 MeV and 5.8 MeV). The detection efficiency of the NaI(Tl) detectors for 19.8 MeV γ-rays can be measured with the help of Li(p,γ) and B(p,γ) reactions using a Van de Graaf's accelerator. To suppress the background in the $pd\mu$ and $pt\mu$ fusion γ-ray spectra the measurements will be carried out in coincidence with muon decay electrons, by demanding that a muon decay be seen after the fusion event, implying that the candidate fusion event was not some other muon disappearance channel (as *e.g.* nuclear capture in gold). The total number of recorded electrons is used as normalization in analysis of the data from different experiments.

The muonic neon X-rays emitted during the cascade will be detected by a germanium detector which provides good energy and time responses. A similar technique has already been applied to measure transfer processes and thereby extract values for the transfer rate from protons to deuterons as well as the rate of formation of the $pp\mu$ molecule [36,42].

Although the apparatus is complex, measurements are comparatively simple, relying on the time of flight principle. The time of muonic deuterium emission is well estimated by the arrival time of the muon, because muonic atom formation, transfer to the deuteron, and emission occur at a rate limited by the transfer time of about 100 ns (for $c_d \sim 10^{-3}$, the transfer rate of μ^- from protium to deuterium is of the order of 10^7 s^{-1}). The flight time is $t_{fl} = x_{fl}/v_{\mu d}$, where $v_{\mu d}$ is the speed at which μd is emitted and $x_{fl} = x_d/\cos\theta$. The angle of emission is θ (which can be limited by collimation), and the separation of the surfaces is x_d. For our case ($x_d = 20$ mm, $\theta = 0°$), we obtain values of t_{fl} ranging from 0.3 to 6.3 μs for $45\ eV \leq E_{d\mu} \leq 0.1\ eV$. The collimator will be used during part of the experiment to determine with most precision the energy of the emitted atoms. The scattering cross-section will be determined from the yields of the muonic neon X-rays and the 5.5 MeV γ-ray. This will be achieved using Monte Carlo simulation calculations.

During the recent measurements of Expt. 613, an emitting layer of 3.5 mg $\cdot$ cm^{-2} of hydrogen with $c_d = 0.1\%$ of D_2 was frozen on the upstream foil. The delayed gold nuclear γ-ray at 356 keV appears after 0.4 μs for the case of an emitting layer upstream. Fig. 9 shows the delayed time spectra of these Au nuclear γ-rays when the downstream gold foil is bare and when it is covered with 1.3 mg $\cdot$ cm^{-2} of pure hydrogen. The reduction in intensity of the amount of μd which reaches the downstream foil is visible and gives a value of (23$\pm$10)%. Monte Carlo simulation predicted a reduction of 25% in intensity. The total count being very low for both measurements, the expected shift in the mean time is not so explicitly visible. This 8-hours measurement shows the feasibility of this type of experiment. Optimizing the experimental conditions as described above will give much better data.

3 Estimates of rates

From Expt. 613 preliminary results and Monte Carlo simulations, we have good estimates about the μd and μt emission yields in vacuum in different experimental conditions of layer thickness and concentration. Because these are very similar for μd and μt we will restrict most of the rate estimates to the muonic deuterium case, unless there exists a discrepancy between μd and μt behaviours. The μt rate estimates will be summarized at the end.

Starting with an incident μ^- rate of 5×10^3 s^{-1} at 27 MeV/c ($\Delta p/p$ = 4% FWHM), approximatively 2×10^3 s^{-1} (40%) of the μ^- will be stopped in 7 mg $\cdot$ cm^{-2} of solid protium-deuterium layer on the upstream gold foil. With a typical deuterium concentration c_d = 0.1%, the probability of having a μd emitted into vacuum and reaching the downstream gold foil at a distance of 20 mm is 2.5% per muon stopped in hydrogen ($\sim$50 s^{-1}). As shown by Fig. 4, the energy of the μd atoms covers a very wide range (0.1 – 45 eV).

When the downstream gold foil is covered only by a thin neon layer of 2 mg $\cdot$ cm^{-2}, all μd reaching the layer will induce a muon transfer reaction to neon atoms. The μNe Lyman series X-rays, produced by transfer, are therefore emitted at $\sim$50 s^{-1}; the μNe (2p-1s) itself will be 40% ($\sim$20 s^{-1}) of the total Lyman series. When adding 2 mg $\cdot$ cm^{-2} of pure protium on top of the neon layer, about half of the μd-atoms ($\sim$25 s^{-1}) are expected to stop there and mostly disappear by formation of $pd\mu$ molecules ($\lambda_{pd\mu} = 5.6 \pm 0.2$ μs^{-1}[30], measured in liquid). This $pd\mu$ will disappear by muon decay, λ_0 =0.45 μs^{-1}, or by fusion ($\lambda_f^{1/2}$=0.35$\pm$0.02 μs^{-1} and $\lambda_f^{3/2}$=0.11$\pm$0.01 μs^{-1} [30]). The probability to obtain a 5.5 MeV γ-ray, taking into account the branching ratio and the statistical population of the spin state, will therefore be about 40% ($\sim$10 s^{-1}). The remaining μd which reach the neon layer will then produce μNe X-rays to a level of $\sim$25 s^{-1}(the μNe (2p-1s) itself will give $\sim$10 s^{-1}). When adding a thicker H_2 layer, about 4 mg $\cdot$ cm^{-2}, almost all the μd will stop in the protium and disappear by formation of $pd\mu$ molecules. Therefore, the 5.5 MeV γ-ray will be emitted to a level of $\sim$20 s^{-1}.

The μNe Lyman series X-ray transition, at energies between 207 and 270 keV will be detected by the Ge detector. The efficiency of these muonic X-rays, taking into account the solid angle of the Ge detector, is estimated to be 0.003. The expected rate for the μNe Lyman series is therefore 9 min^{-1} (the μNe (2p-1s) itself is 3.6 min^{-1}) in the case of a pure neon layer and 4.5 min^{-1} for measurement with the protium layer (1.8 min^{-1} for the μNe (2p-1s) alone). The time resolution of the Ge detector has to be within 10 – 15 ns (FWHM) at $\sim$200 keV in order to allow good energy discrimination of the drifting μd-atoms. For background reduction purposes, we may demand the detection of muon decay electrons following the transfer. The efficiency is approximately 20%. This coincidence makes the acquisition slower, but the data are much cleaner.

The 5.5 MeV γ-ray will be recorded by the NaI(Tl) detectors. They are expected to suffer a strong background due to bremsstrahlung, decay electrons from the beam and other backgrounds, especially neutrons. We do not know yet if these detectors will be able to provide good quality data, so we will present only an optimal case in these initial rates estimates. The downstream NaI(Tl) is not include in the rates here.

The array of four NaI(Tl)-crystals (15 cm diameter each, 15 cm thick) located on one side of the apparatus (see Fig. 2) has a total intrinsic efficiency of 10-15% at 5.5 MeV

and a geometrical acceptance (at a distance of about 50 cm) estimated at 0.02. Hence the typical expected rate of 5.5 MeV γ-rays from $pd\mu$-fusion, occurring downstream with the thick protium layer, is 3.6 min^{-1}. The 5.5 MeV γ-ray produced after $pd\mu$-fusion will be followed (with a probability of 80%) within the next 5 μs by an electron coming from the muon decay. For background reduction and correct signal signature, one asks for a delayed electron coincidence with the 5.5 MeV γ-ray. The geometrical acceptance for the electron counters, located in front of the NaI(Tl) crystals, is 1.5%; the efficiency of the plastic scintillation counters is $\sim$100%. The expected rate after the coincidence is then 2 hour^{-1}. The background level in these NaI(Tl) detectors is very difficult to estimate without making a measurement.

In the case of μt-atoms, the expected rates for the Ge detector are the same as above. The $pt\mu$ molecular formation rates ($\lambda_{pt\mu} = 7.5 \pm 1.0$ μs^{-1} [41], measured in liquid) and the $pt\mu$-fusion rates (λ_f(I=1)=0.07 μs^{-1} [41]) are different than those for the μd. The estimated rate of γ-rays produced by $pt\mu$ fusion at an energy of 19.8 MeV, taking into account the branching ratio and the statistical population of the spin states, is 11% ($\sim$5.5 s^{-1}). The intrinsic efficiency of the NaI(Tl) detectors being 5% at this energy, the expected rate for these γ-rays will be 0.3 min^{-1}. Considering the very low counting rate of 19.8 MeV γ-rays, we may decided to use the MINA crystal for the γ-ray detection in this case. At this stage, we are not sure of the feasibility of this part of the experiment. The possibility of coincidence detection of the 19.8 MeV γ-ray in both the NaI(Tl) and MINA should remove most of the background but maintain $\sim$4 hour^{-1} count rate.

The efficiency curves of both Ge and NaI(Tl) detectors will be calibrated on-line using prompt muonic neon and gold (μAu(2p-1s) X-rays at 5.6 MeV and 5.8 MeV) X-rays. We also plan to use calibration sources off-line to cover the Ge-energy range.

When used, we require from the collimator that it reduces the uncertainty on the time of flight from $\pm$ 30% to $\pm$ 5%. This causes a strong reduction of the μd-emission yield by about a factor of 4, as do the event rates. Dead time losses are less than 20% and have been ignored.

4 Experimental Equipment

The wire chamber array provides tracking information on muon decay electrons. The tracks, when extrapolated to the target, indicate the approximate decay positions. The pair of scintillators located in front of NaI(Tl)-crystals provides trigger, energy and timing informations. The NaI(Tl) crystal array measures the time and energy of fusion γ-rays. A Ge detector will be used to detect muonic neon X-rays. We may have to use gold γ-rays produced by nuclear muon capture. In addition, the Ge detector will be used to check the contamination of the targets by impurities. The ^{4}He cryostat and associated pumping systems keep the gold foils at 3 K to maintain targets of solid hydrogen or neon films.

5 Readiness

The apparatus already exists from Expt. 613 and requires only slight modifications. The modifications concern the design and construction of an efficient shielding for the

NaI(Tl) detectors, and installation of a source of neon. We should be ready by June 1995 for a first run. Considering the complexity of the apparatus and the time required for its installation, it would be preferable to get at three weeks of beam period at a time.

6 Beam Time required

The cryostat and detection system for decay electrons have many separate components and it usually takes at least three or four shifts to align and calibrate to the required precision. Therefore we feel it is inappropriate to assemble the experiment for a running period of less than 36 consecutive shifts (three weeks).

One 36-shift period will be devoted to the measurement of the processes involved after the emission of μd-atoms in vacuum, *i.e.* determination of the scattering of μd-atoms on hydrogen molecules and of the molecular formation rate of the $pd\mu$-molecule. These are differential measurements because we want to study their energy dependance. Complementary measurements have to be achieved:

1. To insert a collimator to measure the "real" energy distribution of the μd-atoms, not the longitudinal one as we did in Expt. 613.
2. Thick protium (in order to hinder μd-atoms passing through) to optimize the 5.5 MeV γ-ray yield.
3. A thin deuterium overlayer upstream in order to change the energy distribution of the muonic deuterium atoms which will reach the downstream target layer and allow us to repeat some of the measurements with the varied distribution.

A second running period of 36 shifts will focus on the processes following the emission of muonic tritium in vacuum. The measurements schedule is basically the same.

7 Data Analysis

The main part of offline analysis is done on the TRIUMF cluster and uses standard histograming and fitting routines with some specialized refinements. Final results also rely on comparison with Monte Carlo calculations. With a VAX-based data acquisition system it is possible to use offline analysis programs as the data is collected, so that most of the information contained in the data is available immediately to the experimenters.

References

1. A. Adamczak *et al.*, Muon Catalyzed Fusion **7** (1992) 309.
2. C. Chiccoli *et al.*, Muon Catalyzed Fusion **7** (1992) 87.
3. Muonic Hydrogen Group, "Experiment 613 Safety Report", Triumf 1993 (Unpublished).

4. D.J. Winfield, "Safety assessment for the tritium hazard for Experiment 454, TRIUMF", Safety and Reliability Directorate, Chalk River Nuclear Laboratories (TSAC supporting document 890404).
5. Ya.B. Zeldovich and S.S. Gershtein, Usp. Fiz. Nauk **71** (1960) 581 [Sov. Phys. Uspekhi **3** (1961) 593].
6. L.I. Ponomarev, Muon Catalyzed Fusion **3** (1988) 629.
7. E. Zavattini, In: Muon Physics, **vol. 2** (Weak Interactions), ed. by V.W. Hughes and C.S. Wu (New York and London), 1975.
8. M. Doi *et al.*, Prog. Theor. Phys. **86** (1991) 13.
9. M. Bubak and M.P. Faifman, JINR Preprint, E4-87-464, Dubna, 1987.
10. A. Adamczak and V.S. Melezhik, Muon Catalyzed Fusion **5** (1991) 65.
11. J. Cohen, Muon Catalyzed Fusion **5** (1991) 3.
12. A. Adamczak, Hyperfine Interactions **82** (1(1993) 91.
13. V.S. Melezhik and J. Wozniak, Muon Catalyzed Fusion **7** (1992) 203.
14. V.P. Dzhelepov *et al.*, Zh. Eksp. Teor. Fiz. **49** (1965) 393.
15. A. Bertin *et al.*, Rivista Del Nuovo Cim. **5** (1975) 423.
16. A. Bertin *et al.*, Nuovo Cim. **A 72** (1982) 225.
17. V.M. Bystritsky *et al.*, Zh. Eksp. Teor. Fiz. **87** (1984) 384.
18. V.P. Dzhelepov *et al.*, Zh. Eksp. Teor. Fiz. **47** (1964) 1243.
19. V.P. Dzhelepov *et al.*, Zh. Eksp. Teor. Fiz. **50** (1966) 1235.
20. J. Kraiman *et al.*, Phys. Rev. Let. **63** (1989) 1942.
21. J. Kraiman *et al.*, Muon Catalyzed Fusion **5** (1991) 43.
22. D.J. Abbott *et al.*, Proceedings of Ascona Workshop on Muonic Atoms and Molecules, Ascona, April 5-9, 1992, Birkhäuserverlag, Basel, p. 243.
23. A. Adamczak *et al.*, to be published.
24. L.W. Alvarez *et al.*, Phys. Rev. **105** (1957) 1127.
25. V.E. Markushin *et al.*, Hyperfine Interaction **82** (1993) 373.
26. M. Schiff, Nuovo Cim. **22** (1961) 66.
27. S. Cohen *et al.*, Phys. Rev. **119** (1960) 397.
28. E.J. Bleser *et al.*, Phys. Rev. **132** (1963) 2679.
29. V.M. Bystritsky *et al.*, Zh. Eksp. Teor. Fiz. **43** (1976) 606.
30. C. Petitjean *et al.*, Muon Catalyzed Fusion **5** (1991) 199.

31. P. Bauman *et al.*, Muon Catalyzed Fusion **5** (1991) 87.

32. G.M. Marshall, "TRIUMF proposal 453: Production of Slow Muonic Hydrogen in Vacuum".

33. G.M. Marshall, "TRIUMF proposal 613: Reactions of Muonic Hydrogen Isotopes".

34. P.E. Knowles *et al.*, presented at the International Workshop on Muon Catalyzed Fusion, μCF-92, Uppsala, June 28-July 3, 1992, Hyperfine Interactions **82** (1993) 521.

35. G.M. Marshall *et al.*, presented at the International Workshop on Muon Catalyzed Fusion, μCF-92, Uppsala, June 28-July 3, 1992, Hyperfine Interactions **82** (1993) 529.

36. R. Jacot-Guillarmod *et al.*, presented at the International Workshop on Muon Catalyzed Fusion, μCF-92, Uppsala, June 28-July 3, 1992, Hyperfine Interactions **82** (1993) 501.

37. L.I. Ponomarev and M.P. Faifman, Sov. Phys. JETP **44** (1976) 886.

38. M.C. Fujiwara, M.A.Sc. thesis, University of British Columbia, 1994 (unpublished).

39. V.M. Bystritsky *et al.*, Sov. Phys. JETP **44** (1976) 881.

40. P. Ackerbauer *et al.*, Hyperfine Interaction **82** (1993) 243, and references therein.

41. F.J. Hartmann *et al.*, Hyperfine Interaction **82** (1993) 259.

42. R. Jacot-Guillarmod *et al.*, presented at the Ascona Workshop on Muonic Atoms and Molecules, Ascona, April 5-9, 1992, Birkhäuserverlag, Basel, p. 261.

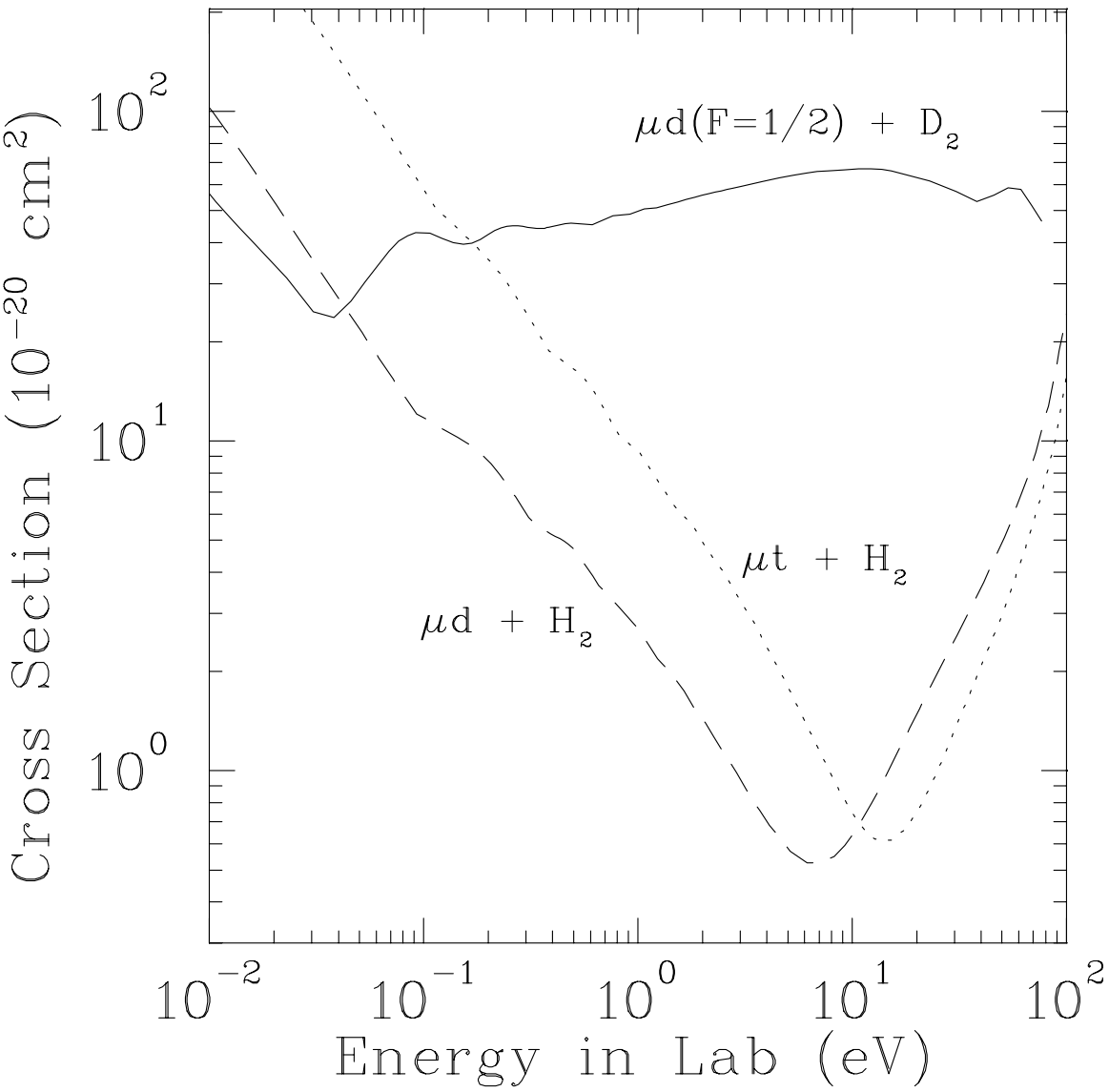

Fig. 1 Elastic scattering cross sections for μd and μt atoms colliding with hydrogen molecules. Note the Ramsauer-Townsend minimum for energy between 2 and 20 eV/@. For comparison, the scattering cross section for μd in the hyperfine state $F = \frac{1}{2}$ on deuterium molecules is shown. These calculations are valid for a hydrogen target between 3 and 30 K.

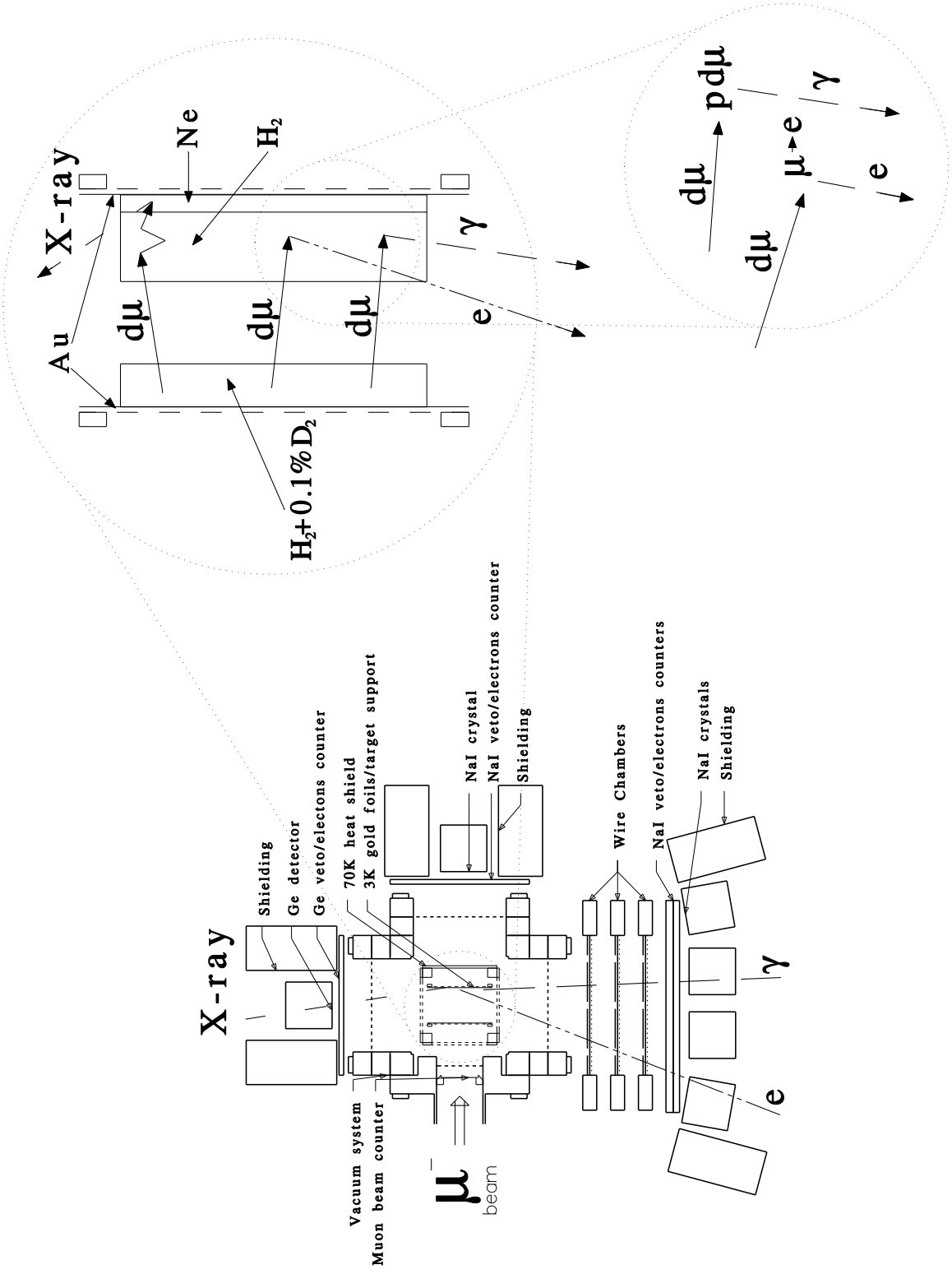

Fig. 2 Arrangement of the solid hydrogen target system, showing the detector positions (top view) and a schematic view of the muonic processes of interest.

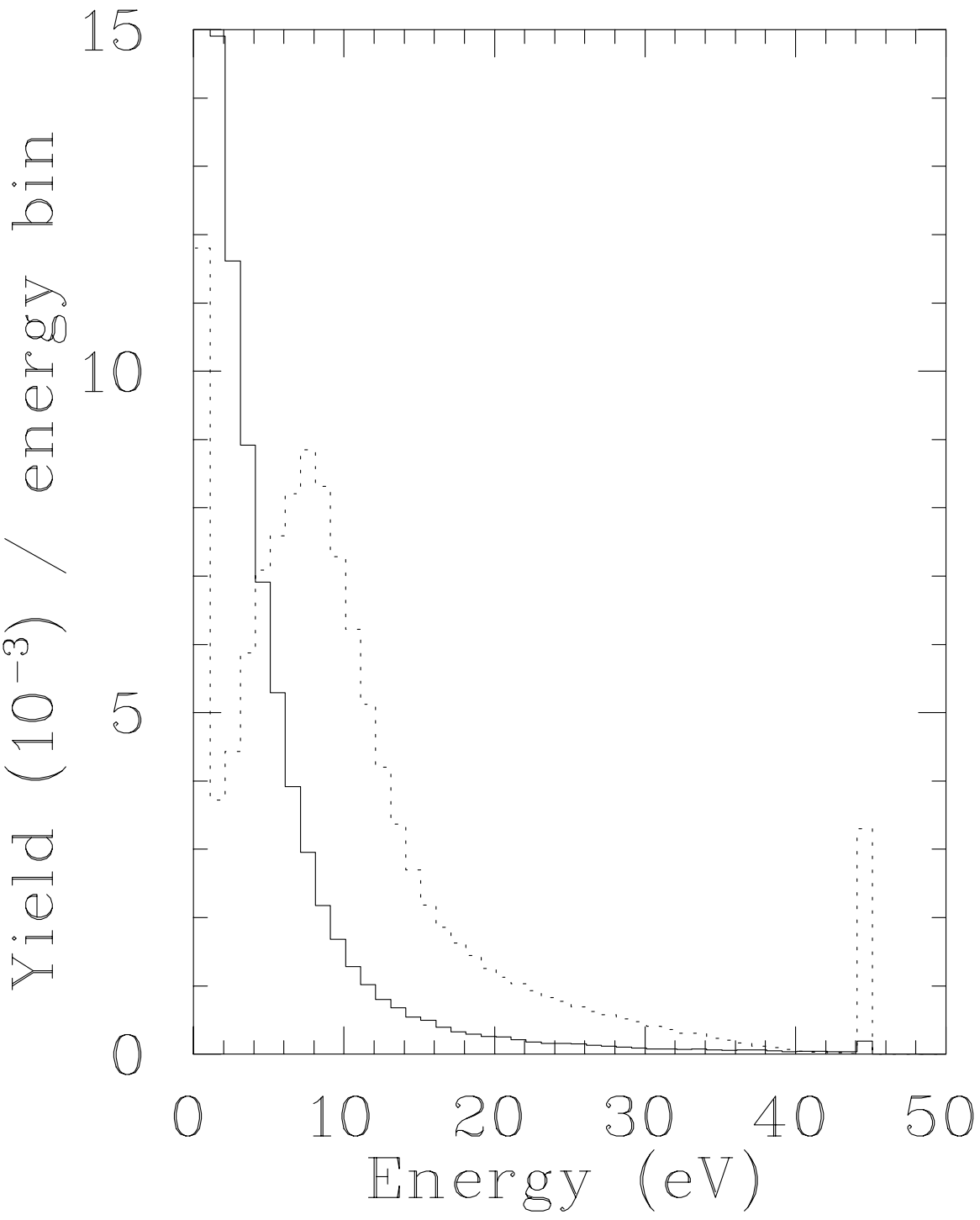

Fig. 3 Monte Carlo simulated energy spectra of μt atoms when they leave the emission layer of 7.0 mg $\cdot$ cm^{-2} solid H_2 with c_t = 0.1% T_2 (dotted line) and when the emission layer is covered by a thin 20 μg $\cdot$ cm^{-2} solid D_2 overlayer (solid line).

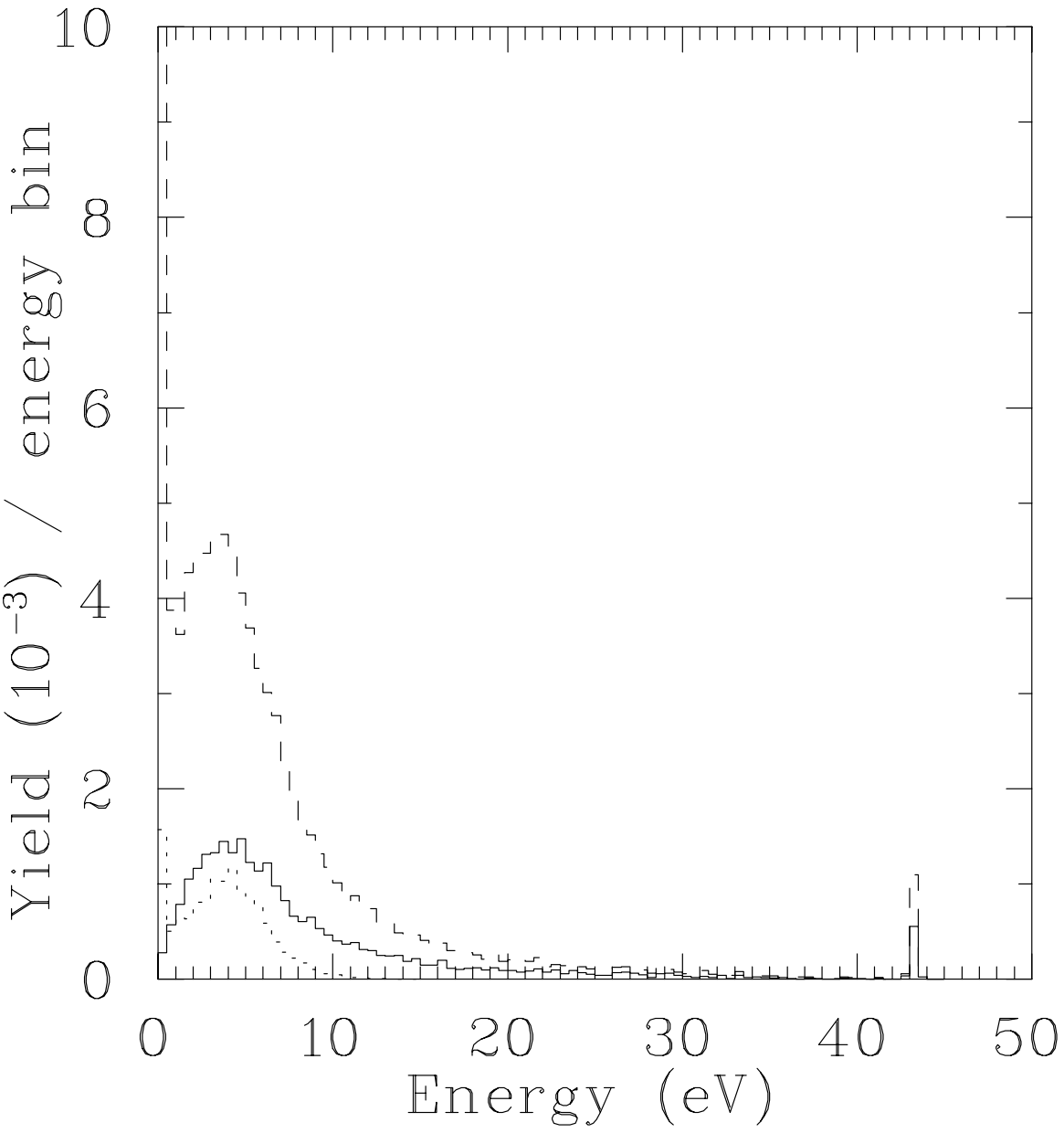

Fig. 4 Monte Carlo simulated energy spectra of μd atoms when they leave the emission layer (dashed line) and when they reach the downstream neon layer with (dotted line) and without (solid line) a protium overlayer of 2.1 $\mathrm{mg \cdot cm^{-2}}$ thickness.

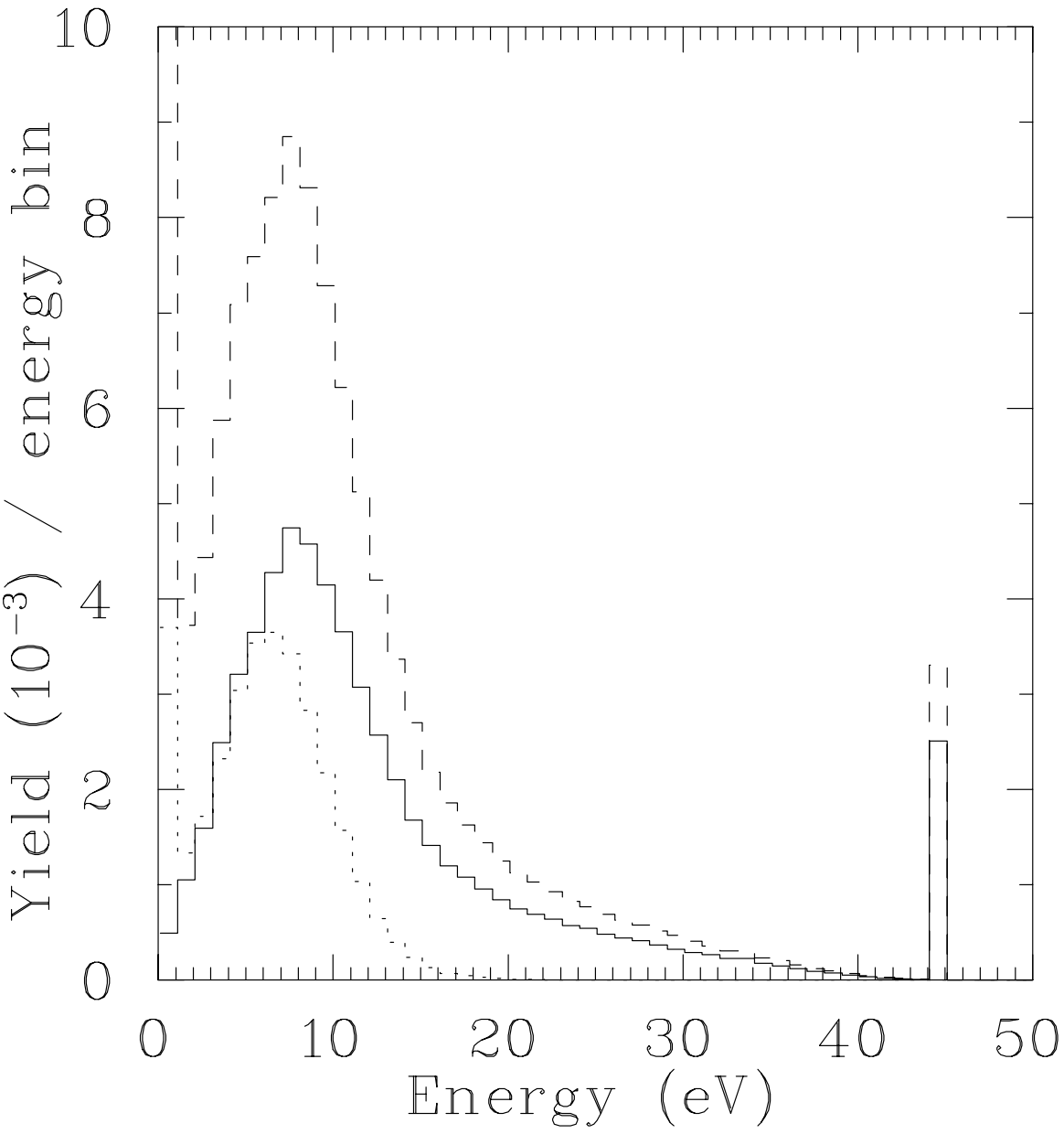

Fig. 5 Monte Carlo simulated energy spectra of μt atoms when they leave the emission layer (dashed line) and when they arrive downstream with (dotted line) and without (solid line) hydrogen (2.0 mg $\cdot$ cm^{-2}) on top of the neon layer.

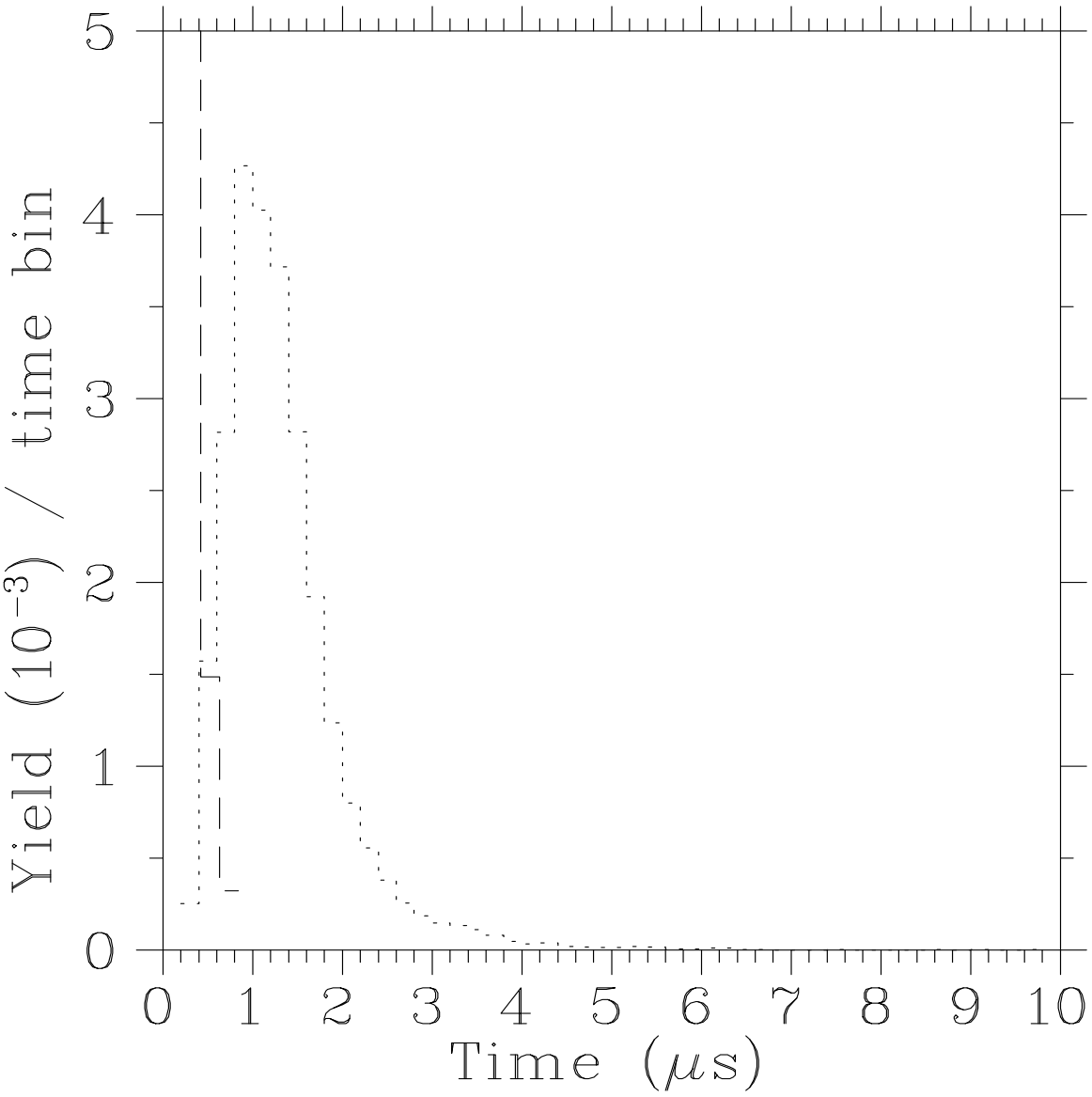

Fig. 6 Monte Carlo simulated time spectra of μd emission times (dashed line) and arrival times at the downstream foil without collimator (dotted line).

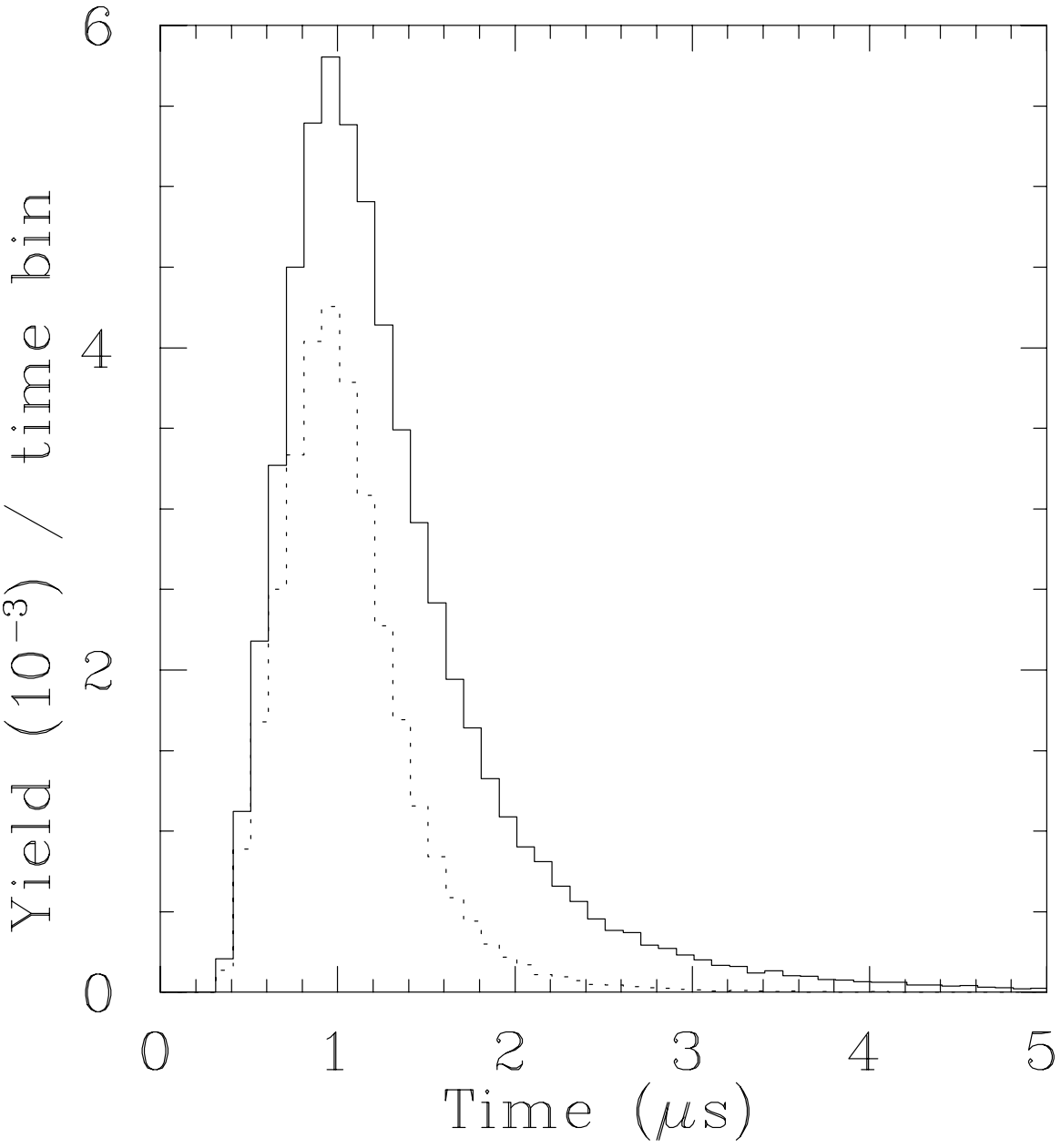

Fig. 7 Monte Carlo simulated time spectra of μNe X-rays produced after transfer from μt atoms, with (dotted line) and without (solid line) hydrogen (2.0 mg $\cdot$ cm^{-2}) on top of the downstream neon layer.

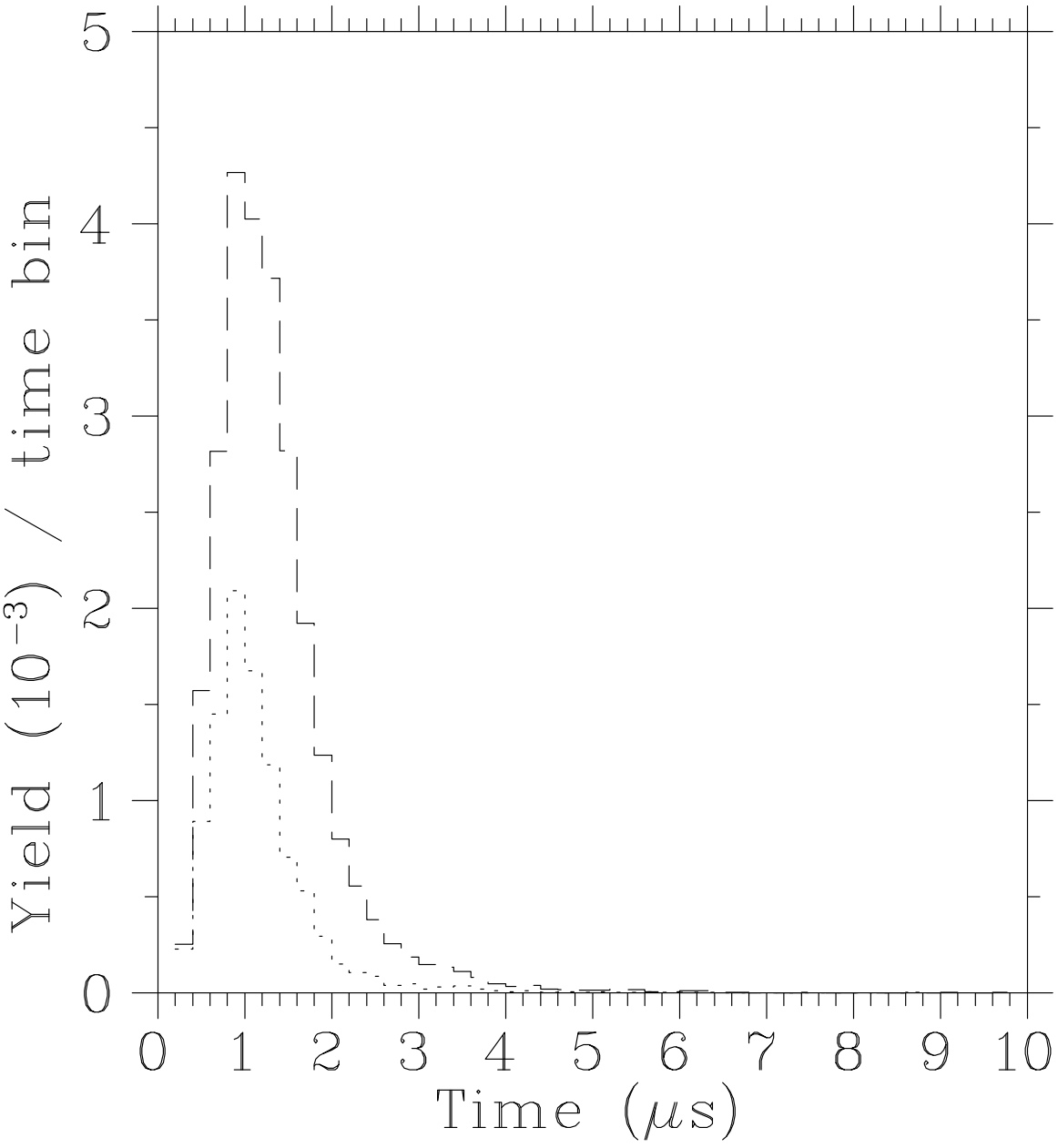

Fig. 8 Monte Carlo simulated time of μd escaping the emission layer and reaching the downstream foil with (dotted line) and without (dashed line) the collimator. The collimator full acceptance angle is $\pm 15°$.

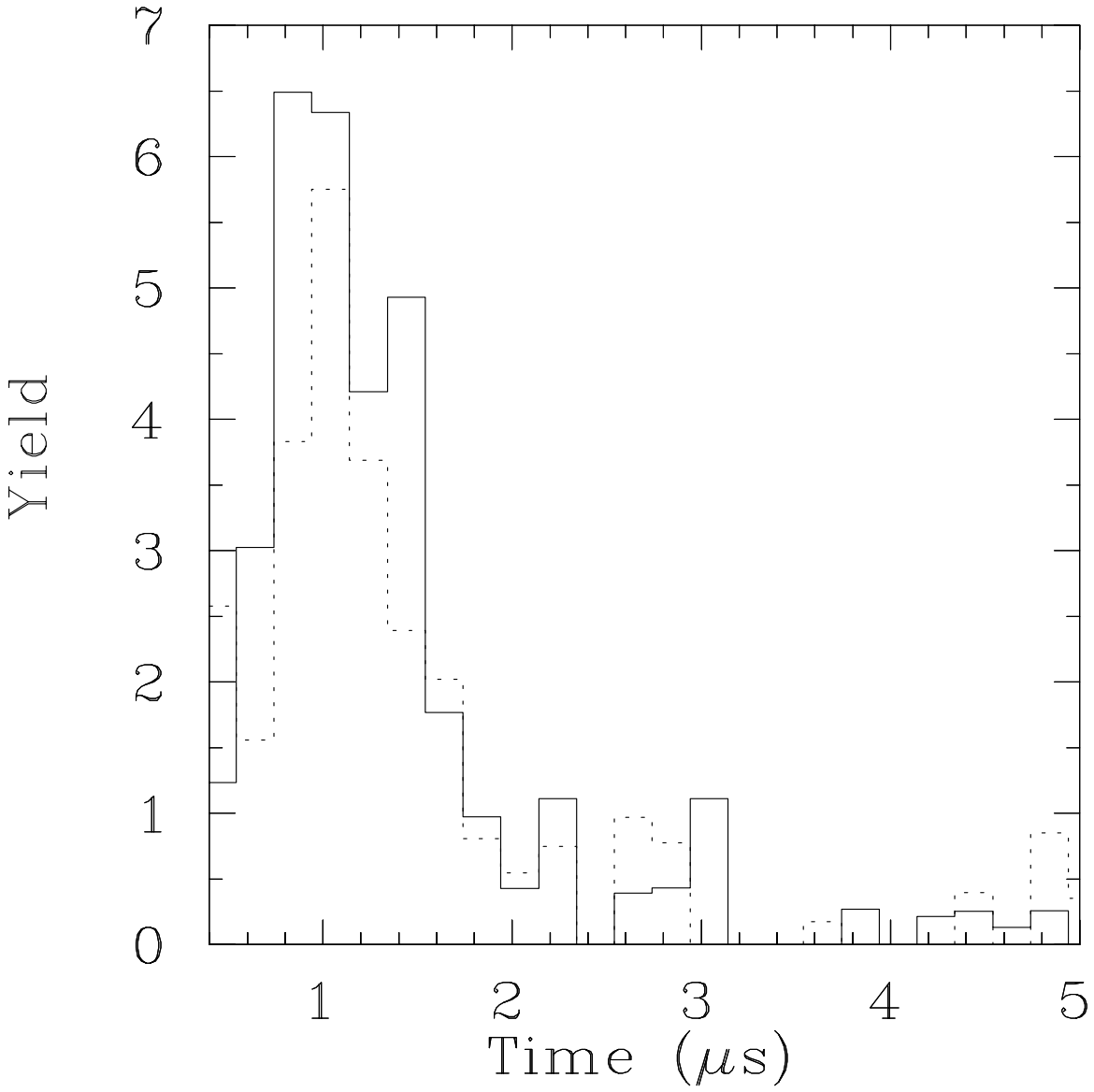

Fig. 9 Measured time spectra of Au nuclear γ-rays at 356 keV in two different measurements, with (dotted line) and without (solid line) 1.3 mg $\cdot$ cm^{-2}hydrogen overlayer on the downstream gold foil. The bin size is 200 ns and the detector time resolution is about 20 ns.

Include publications in refereed journal over at least the previous 5 years.

1. A. Bertin, M. Bruschi, V.M. Bystritsky *et al.*, *Performance of a coincidence neutron spectrometer with double pulse-shape discrimination*, NIM **A 337** (1994) 445.

2. V.M. Bystritsky, A.V. Kravtsov, J. Rak, *Experimental estimates of rates of muon transfer from excited pμ-atoms to helium nuclei*, Kerntechnik **58** (1993) 185.

3. A. Bertin, M. Bruschi, D. Bulgarelli, V.M. Bystritsky *et al.*, *Neutron spectrometry by means of a two-stage neutron-γ pulse-shape discriminating apparatus*, Nuovo Cim. **A 105** (1992) 751.

4. V.M. Bystritsky *et al.*, *Investigation of hydrogen permeability of protective coating for high-temperature alloy EI698*, JINR Communication P13-91-128, Dubna, 1991; Atomnaya Energiya **73** (1992) 354.

5. S. Affatato, A. Bertin, M. Bruschi, D. Bulgarelli, V.M. Bystritsky *et al.*, *Neutron background determination in the Gran Sasso Laboratory by means of a novel coincidence neutron spectrometer*, Nuovo Cim. **A 104** (1991) 437.

6. S. Affatato, A. Bertin, M. Bruschi, D. Bulgarelli, V.M. Bystritsky *et al.*, *Measurement of a very low neutron background within a significant γ-ray environment by means of a coincidence spectrometer with n-γ pulse shape discrimination*, in Proceedings of Int. Progress Rev. on Anomalous Nuclear Effects in Deuterium-Solid Systems, BYU, October 22-23, 1990, AIP Conf. Proc. **228** (1991) 3.

7. V.V. Latyshev, V.M. Bystritsky *et al.*, *Interaction hydrogen isotopes with membranes from palladium alloys*, Fizika Metallov i Metallovedenie **6** (1991) 5.

8. M. Bubak, V.M. Bystritsky, *Cycle-by-cycle time distribution of muon catalyzed fusion registered omitting events with signatures in deadtime intervals*, Kerntechnik **56** (1991) 215.

9. V.M. Bystritsky, V.A. Stolupin, *On the experimental determination of parameters of hydrogen-isotope μ-atom charge exchange on He nuclei*, J. of Nucl. Phys. **53** (1991) 1005.

10. V.M. Bystritsky *et al.*, *Kinetics of mesic hydrogen in hydrogen-helium mixtures*, Muon Catalyzed Fusion **5/6** (1990/1991) 487.

11. V.M. Bystritsky, A.V. Kravtsov, N.P. Popov, *Kinetics of the excited muonic hydrogen in the mixtures of hydrogen isotopes and helium*, Zhur. Eksp. Teor. Fiz. **97** (1990) 73.

12. V.M. Bystritsky *et al.*, *Study of the process of muon transfer from dμ-atoms to He in deuterium-helium mixture at pressure 1350 atm*, Zhur. Eksp. Teor. Fiz. **98** (1990) 1514.

13. V.M. Bystritsky *et al.*, *Measurement of the temperature dependence of the ddμ-molecule formation rate in gaseous deuterium at the pressure 1.5 and 0.4 kbar*, Muon Catalyzed Fusion **5/6** (1990/1991) 141.

14. V.M. Bystritsky *et al.*, *A membrane filter for diffusional separation and production of ultra-pure hydrogen isotopes*, Prib. Tekh. Eksp. **1** (1990) 216.

15. V.M. Bystritsky *et al.*, *The study of the effect of surface alluminizing on hydrogen penetration through target wall at high pressures and temperatures*, Atomnaya Energiya **69** (1990) 101.

16. V.M. Bystritsky *et al.*, *Investigation of hydrogen isotope penetration through stainless steels*, Atomnaya Energiya **66** (1989) 413.

17. A.P. Arkhipov, V.M. Bystritsky *et al.*, *Target for operation with hydrogen heavy isotopes of pressure up to 1000 atm and temperatures up to 1050 K*, Prib. Tekh. Eksp. **6** (1989) 47.

18. V.M. Bystritsky *et al.*, *A high pressure bellow valve*, Prib. Tekh. Eksp. **4** (1989) 212.

19. V.M. Bystritsky *et al.*, *A target for work with hydrogen isotopes at pressures up to 1500 atm in the temperature range from 20.4 to 300 K*, Prib. Tekh. Eksp. **1** (1989) 50.

20. V.M. Bystritsky *et al.*, *The measurement of ddμ-molecule formation rate at high deuterium pressure (0.4-1.5 kbar)*, in: AIP Conf. Proceedings **181** (1988) 17.

21. V.M. Bystritsky, *The scattering of muonic atoms in hydrogen isotopes. Status and proposals*, to be published in "Nukleonika".

22. V.M. Bystritsky, *Review of experimental results for muon transfer from hydrogen to helium*, to be published in "Nukleonika".

23. V.M. Bystritsky *et al.*, *A Monte Carlo study of fast neutron registration efficiency by multichannel system NE213-detectors*, to be published in "Nukleonika".

24. V.M. Bystritsky *et al.*, *Calculation of neutron registration efficiency by the coincidence spectrometer with Li-glass scintillator*, to be published in "Nukleonika".

25. V.M. Bystritsky, *On measurement of cross sections for scattering of pμ- and dμ-atoms in hydrogen and deuterium*, JINR Preprint, E1-93-450, Dubna, 1993 (to be published in "Yadernaya Fizika").

26. V.M. Bystritsky, *Muon transfer from muonic atoms of hydrogen isotopes to He nuclei. Status and proposals*, JINR Preprint, E1-93-451, Dubna, 1993 (to be published in "Yadernaya Fizika").

27. V.B. Belyaev, V.M. Bystritsky *et al.*, *New proposals for the investigation of strong interaction of light nuclei at super low energies*, to be published in "Nukleonika".

28. R. Jacot-Guillarmod *et al.*, *Comparison of muon and pion capture ratios in H_2-Ar gas mixtures*, Phys. Rev. **A 39** (1989) 387.

29. R. Jacot-Guillarmod, *Muonic X-ray intensities and electronic structure in elements with $5<Z<20$*, Muon Catalyzed Fusion **4** (1989) 113.

30. F. Mulhauser, H. Schneuwly, R. Jacot-Guillarmod *et al.*, *Charge transfer from muonic hydrogen to sulphur and oxygen in a H_2 + SO_2 gas mixture*, Muon Catalyzed Fusion **4** (1989/1991) 365.

31. R. Jacot-Guillarmod, F. Mulhauser *et al.*, *Charge transfer from muonic hydrogen to neon*, Phys. Rev. Lett. **65** (1990) 709.

32. C. Piller, C. Gugler, R. Jacot-Guillarmod *et al.*, *Nuclear charge radii of tin isotopes from muonic atom*, Phys. Rev. **C 42** (1990) 182.

33. F. Mulhauser, R. Jacot-Guillarmod *et al.*, *Charge transfer from muonic hydrogen to elements with 8<Z<18*, Muon Catalyzed Fusion **5/6** (1990/1991) 101.

34. G.M. Marshall, J.M. Bailey, G.A. Beer, J.L. Beveridge, J.H. Brewer, B.M. Forster, W.N. Hardy, T.M. Huber, R. Jacot-Guillarmod *et al.*, *Reactions of muonic hydrogen isotopes*, Z. Phys. **C 56** (1992) S44.

35. H. Schneuwly and F. Mulhauser, *Ephemeral muonic hydrogen atoms*, Phys. Lett. **A 160** (1991) 71, **162** (1992) 506.

36. G. Fricke, J. Herberz, T. Hennemann, G. Mallot, L.A. Schaller, L. Schellenberg, C. Piller and R. Jacot-Guillarmod, *Behavior of nuclear charge radii systematics in the s-d shell from muonic atom measurements*, Phys. Rev. **C 45** (1992) 80.

37. F. Mulhauser and H. Schneuwly, *Muon transfer to sulphur dioxide* J. Phys. B: At. Mol. Opt. Phys. **26** (1993) 4307.

38. R. Jacot-Guillarmod *et al.*, *Muon transfer from hot muonic hydrogen atoms to neon*, Hyperfine Interactions **82** (1993) 501.

39. G.M. Marshall, J.M. Bailey, G.A. Beer, J.L. Beveridge, J.H. Brewer, B.M. Forster, T.M. Huber, R. Jacot-Guillarmod *et al.*, *Experiments with energetic muonic μd and μt atoms emitted from solid hydrogen*, Hyperfine Interactions **82** (1993) 529.

40. P.E. Knowles, G.A. Beer, G.R. Mason, A. Olin, J.M. Bailey, J.L. Beveridge, G.M. Marshall, J.H. Brewer, B.M. Forster, T.M. Huber, R. Jacot-Guillarmod *et al.*, *Producing $\mu^- d$ and $\mu^- t$ in Vacuum*, Hyperfine Interactions **82** (1993) 521.

41. F. Mulhauser and H. Schneuwly, *Systematic study of muon transfer to sulphur dioxide*, Hyperfine Interaction **82** (1993) 507.

42. J.C. Staško, B. Bassalleck, E.C. Booth, M.B. Chertok, D. Healey, R. Jacot-Guillarmod *et al.*, *Radiative Decay of the Δ Resonance : Analyzing Powers for $\pi^- \vec{p} \to \gamma n$*, Phys. Rev. Lett. **72** (1994) 973.